

# Size-scale effects on minimum flexural reinforcement in RC beams: application of the cohesive crack model

E. Cadamuro, M. Corrado & A. Carpinteri  
*Politecnico di Torino, Torino, Italy*

**ABSTRACT:** The prescriptions provided by the codes of practice for the assessment of the minimum reinforcement amount in reinforced concrete beams usually disregard the nonlinear contribution of concrete in tension and the size-scale effects. In the present paper, these phenomena are correctly taken into account in the description of the flexural failure in lightly reinforced concrete beams by means of a numerical algorithm based on Nonlinear Fracture Mechanics. In this context, the application of Dimensional Analysis permits a reduction in the number of the governing parameters. In particular, it is analytically demonstrated that only two nondimensional parameters,  $N_P$  and  $s$ , are responsible for the brittle-to-ductile transition in the mechanical response. According to this approach, a new formula suitable for the evaluation of the minimum reinforcement in practical applications is proposed. A comparison with experimental results demonstrates the effectiveness of the proposed model.

## 1 INTRODUCTION

### 1.1 *Standard Codes Provisions*

The Limit Analysis of reinforced concrete (RC) beams usually assumes that stretched concrete is not bearing load and so the cracking phenomenon is not taken into account in the evaluation of the load carrying capacity. This assumption not always yields to a safe design condition, as for instance in the case of lightly reinforced concrete beams, where the tensile concrete contribution determines a hyper-strength with respect to the ultimate loading condition, with a consequent possible instability in the overall mechanical response. In this case, in fact, the resistant bending moment after the peak cracking moment is a monotonic decreasing function of the crack length, due to an unstable fracture propagation. For this reason, all national and international standard codes of practice provide empirical formulas for the determination of the minimum reinforcement amount which enables RC members to prevent unstable crack propagation. Most of them consider only two parameters: the concrete grade and the steel yield strength, whereas other important parameters, such as the size-scale, are completely neglected. As an example, Model Code 90 (1993) and British Standards BS 8110-1 (1997) give values of minimum reinforcement depending only on the steel grade, whereas Eurocode 2 (2004) and ACI 318-05 (2005) provide values of minimum reinforcement proportional to the concrete compressive strength and in inverse relation to the steel yield strength. Only the

Norwegian Standards NS 3473 E (1989) accounts for the effect of the member size, by means of the size-effect factor,  $k_w$ , equal to  $1.5-h/h_1 \geq 1$ , where  $h$  is the beam depth in m, and  $h_1$  is equal to 1 m. Finally, the Australian Standards AS 3600 (2001) consider the minimum reinforcement as a function of the ratio of overall to effective beam depth,  $D/d$ .

### 1.2 *Models for Computing Minimum Reinforcement*

A more accurate assessment of the minimum reinforcement taking into account the size-scale effects should be accomplished in order to save steel reinforcement and money in case of large structures. To this aim, most of the models available in the literature propose detailed analysis taking into account the complex behavior due to fracture propagation in tension, on the basis of Linear and Nonlinear Fracture Mechanics approaches (Ghali et al. 1986, Baluch et al. 1992, Gerstle et al. 1992, Fantilli et al. 1999, Ruiz et al. 1999, Appa Rao et al. 2007).

In this context, significant contributions derive from the application of the *Bridged Crack Model* (Carpinteri 1981a, 1984, Bosco & Carpinteri 1992), which is based on Linear Elastic Fracture Mechanics, to the study of the crack propagation in presence of a reinforcement. According to this model, the overall response of RC beams can be described by means of the reinforcement brittleness number,  $N_P$ , obtained through Dimensional Analysis on the basis of the mechanical and geometrical properties (Carpinteri 1981a, 1984):

$$N_p = \rho \frac{\sigma_y h^{0.5}}{K_{IC}} \quad (1)$$

where  $\sigma_y$  is the steel yield strength,  $h$  is the beam depth,  $K_{IC}$  is the concrete toughness, and  $\rho$  is the reinforcement percentage. A ductile behavior is predicted for high values of  $N_p$ , whereas a brittle response is expected for low values of  $N_p$ . In particular, it is possible to define  $N_{PC}$ , as the critical value which separates the brittle response from the ductile one, corresponding to the minimum reinforcement amount condition. The value  $N_{PC} = 0.26$  was experimentally obtained by Bosco et al. (1990) for high strength concrete beams, and, subsequently, the following empirical equation has been proposed by Bosco & Carpinteri (1992) to express the dependence of  $N_{PC}$  on the concrete grade  $\sigma_c$ :

$$N_{PC} = 0.1 + 0.0023\sigma_c \quad (2)$$

Equating the expression of  $N_p$  (Eq. (1)) to that of  $N_{PC}$  (Eq. (2)) and solving with respect to  $\rho$ , the following formula for the minimum reinforcement amount is obtained:

$$\rho_{\min} = \frac{K_{IC}}{\sigma_y h^{0.5}} (0.1 + 0.0023\sigma_c) \quad (3)$$

In the present paper, Dimensional Analysis is applied to the algorithm proposed by Carpinteri et al. (2007) based on the *Cohesive* and the *Overlapping Crack* models in the specific case of lightly reinforced concrete beams in bending. It will be demonstrated that two nondimensional parameters,  $N_p$  and  $s$ , are responsible for the mechanical behavior, and not  $N_p$  only, as considered so far. Finally, on the basis of these two brittleness number a new formula will be proposed for the evaluation of the minimum reinforcement amount.

## 2 THE INTEGRATED COHESIVE AND OVERLAPPING CRACK MODEL

Let us consider the reinforced concrete beam element in Figure 1 with a rectangular cross-section of thickness  $b$  and depth  $h$ , a steel reinforcement layer distant  $c$  from the lower edge and a crack length  $a$ . The beam segment has a length  $l$  equal to the depth and is subjected to the external bending moment  $M$ . We assume that the middle cross-section can be considered as representative of the mechanical behavior of the whole element, since all the mechanical nonlinearities due to cracking in tension, steel yielding and crushing of concrete in compression, are lo-

calized in this section, whereas the outside parts exhibit an elastic response.

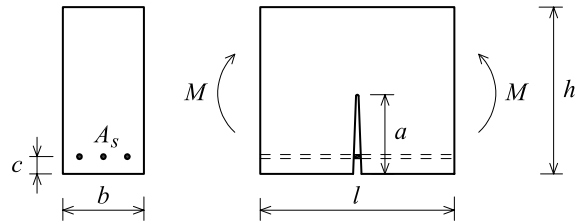


Figure 1. Scheme of the reinforced concrete element.

### 2.1 Constitutive Models

The mechanical response of concrete in tension is described by the *Cohesive Crack Model* (Hillerborg et al. 1976, Carpinteri 1985). In particular, a linear-elastic stress-strain relationship is assumed for the undamaged phase, whereas a softening stress-crack width relationship describes the process zone up to the critical opening,  $w_{cr}^t$ , is reached (Fig. 2). The softening function,  $\sigma = f(w)$ , is considered as a material property, as well as the critical value of the crack opening,  $w_{cr}^t$ , and the fracture energy,  $G_F$ . The shape of  $f(w)$  may vary from linear to bilinear or even more complicated relationships depending on the characteristics of the considered material and the analyzed problem. Recently, a general polynomial relationship with fractional or integer powers has been proposed to express all known cohesive crack laws for concrete (Karihaloo & Xiao 2008).

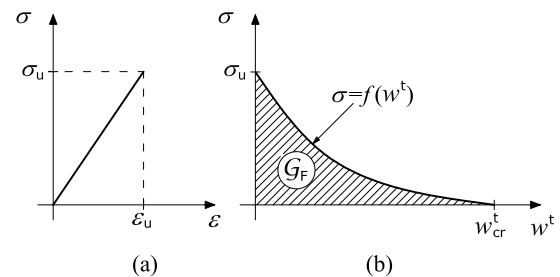


Figure 2. Cohesive Crack Model: (a) linear-elastic  $\sigma$ - $\epsilon$  law; (b) post-peak softening  $\sigma$ - $w$  relationship.

As far as modeling of concrete crushing failure is concerned, the *Overlapping Crack Model* introduced by Carpinteri et al. (2007, 2009) is adopted. According to such an approach, strongly confirmed by experimental results (van Mier 1984, Jansen & Shah 1997), and derived from the pioneering work by Hillerborg (1990), the inelastic deformation in the post-peak regime is described by a fictitious interpenetration of the material, while the remaining part of the specimen undergoes an elastic unloading. A pair of constitutive laws is introduced, in close analogy with the *Cohesive Crack Model*: a stress-strain relationship until the compressive strength is

achieved (Fig. 3a), and a stress-displacement (overlapping) relationship describing the phenomenon of concrete crushing (Fig. 3b). The latter law, usually assumed as a linear decreasing function, describes how the stress in the damaged material decreases from its maximum value down to zero as the fictitious interpenetration increases from zero to the critical value,  $w_{cr}^c$ . It is worth noting that the crushing energy,  $G_C$ , which is a dissipated surface energy, defined as the area below the post-peak softening curve in Figure 3b, can be assumed as a true material property, since it is almost independent of the structural size. An empirical equation for calculating the crushing energy has been recently proposed by Suzuki et al. (2006), taking into account the lateral confinement exerted by stirrups.

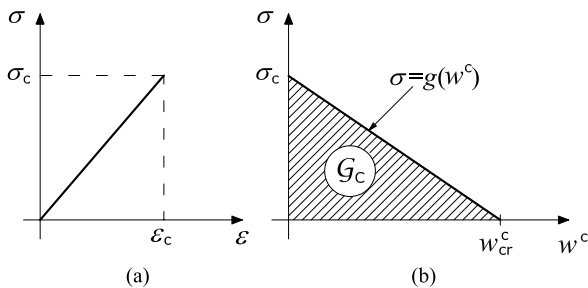


Figure 3. Overlapping Crack Model: (a) linear-elastic  $\sigma$ - $\varepsilon$  law; (b) post-peak softening  $\sigma$ - $w$  relationship.

The steel reinforcement contribution is modeled by a stress vs. crack opening relationship obtained by means of preliminary studies carried out on the interaction between the reinforcing bar and the surrounding concrete. On the basis of the bond-slip relationship provided by the Model Code 90 (1993), and by imposing equilibrium and compatibility conditions, it is possible to correlate the reinforcement reaction to the relative slip at the crack edge, which corresponds to half the crack opening displacement. Typically, the obtained relationship is characterized by an ascending branch up to steel yielding, to which corresponds a critical value of the crack opening,  $w_y$ . After that, the steel reaction is nearly constant.

## 2.2 Numerical Algorithm

The numerical model herein proposed to describe the fracturing behavior of lightly reinforced concrete beams is derived from the more general algorithm introduced by Carpinteri et al. (2007, 2009) for modeling the mechanical response of all the possible situations ranging from plain to over-reinforced concrete beams. The proposed model, in fact, permits to correctly describe the relevant nonlinearities. Similar approaches have been proposed by Carpinteri (1985), Planas & Elices (1992), Bažant & Beissel

(1994) and Brincker et al. (1999) to model a cohesive crack in plain and reinforced concrete beams.

The mid-span cross-section of the considered element is subdivided into  $n$  nodes, where cohesive and overlapping stresses are replaced by equivalent nodal forces,  $F_i$ , which depend on the corresponding relative nodal displacements according to the cohesive or overlapping post-peak laws (Fig. 4a). The following relationship holds between the horizontal forces,  $F_i$ , and the horizontal displacements,  $w_j$ :

$$\{F\} = [K_w]\{w\} + \{K_M\}M \quad (4)$$

where  $[K_w]$  is the matrix of the coefficients of influence for the nodal displacements, and  $\{K_M\}$  is the vector of the coefficients of influence for the applied moment  $M$ , computed a priori by a finite element analysis.

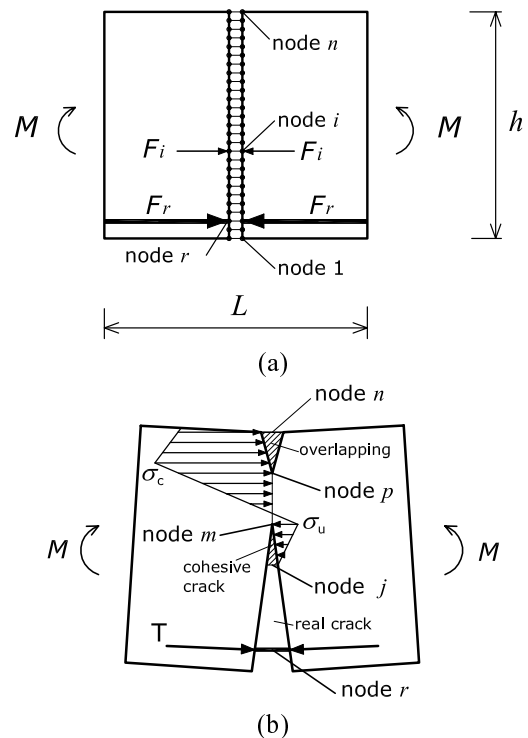


Figure 4. Finite element nodes (a); and force distribution with cohesive crack in tension, crushing in compression and reinforcement closing forces (b) across the mid-span cross-section.

Equation (4) constitutes a linear algebraic system of  $(n)$  equations and  $(2n+1)$  unknowns,  $\{F\}$ ,  $\{w\}$  and  $M$ . With reference to the generic situation reported in Figure 4b,  $n$  additional equations can be introduced by considering the constitutive laws for concrete in tension and compression and for the reinforcement in the node  $r$  (see Carpinteri et al. 2007, 2009 for more details). The last additional equation derives from the strength criterion adopted to govern the propagation processes. We can set either the force in the fictitious crack tip,  $m$ , equal to the ultimate tensile force,  $F_u$ , or the force in the fictitious

crushing tip,  $p$ , equal to the ultimate compressive force,  $F_c$ . It is important to note that cracking and crushing phenomena are physically independent of each other. As a result, the situation which is closer to one of these two possible conditions is chosen to establish the prevailing phenomenon. The driving parameter of the process is the position of the fictitious tip that in the considered step has reached the limit resistance. Finally, at each step, we can compute the rotation,  $\mathcal{G}$ :

$$\mathcal{G} = \{D_w\}^T \{w\} + D_M M \quad (5)$$

where  $\{D_w\}$  is the vector of the coefficients of influence for the nodal displacements, and  $D_M$  is the coefficient of influence for the applied bending moment,  $M$ . The size-scale effects are taken into account by means of relationships of proportionality that affect the coefficients of influence entering Eqs. (4) and (5).

### 3 APPLICATION OF DIMENSIONAL ANALYSIS TO LIGHTLY RC BEAMS

The most relevant applications of Dimensional Analysis in Solids Mechanics have concerned complete and incomplete physical similarity of strength and toughness in disordered materials (Carpinteri 1980, 1981b, 1984, Phatak & Dhonde 2003, Phatak & Deshpande 2005), as well as the study of the incomplete self-similarity in fatigue crack growth (Barenblatt & Botvina 1980, Ciavarella et al. 2008).

When the flexural behavior of reinforced concrete beams is studied, according to the numerical model proposed in the previous section, the functional relationship among the quantities that characterize the phenomenon is the following:

$$M = \Phi(\sigma_u, G_F, \sigma_c, G_C, E_c, \sigma_y, \rho_t, h; b/h, l/h, \mathcal{G}) \quad (6)$$

where  $M$  is the resistant bending moment,  $\sigma_u$ ,  $G_F$ ,  $\sigma_c$ ,  $G_C$ ,  $E_c$  are, respectively, the tensile strength, the fracture energy, the compressive strength, the crushing energy, and the elastic modulus of concrete,  $\sigma_y$  and  $\rho_t$  represent the yielding strength and the percentage of the tensile reinforcement,  $h$  is the characteristic size of the body,  $b/h$  and  $l/h$  define the geometry of the sample according to Figure 1, and  $\mathcal{G}$  is the local rotation of the element. Since we are interested in the mechanical response of lightly reinforced concrete beams, the set of variables can be reduced as follows:

$$M = \Phi(\sigma_u, G_F, E_c, \sigma_y, \rho_t, h; \mathcal{G}) \quad (7)$$

where the parameters describing the behavior of concrete in compression,  $\sigma_c$  and  $G_C$ , are not explicitly considered, since the crushing failure is not involved in the failure mechanism. On the other hand, only the beam depth,  $h$ , is considered if the geometrical ratios of the samples,  $b/h$  and  $l/h$ , are assumed to be constant. The application of Buckingham's  $\Pi$ -Theorem (Buckingham 1915) for physical similitude and scale modeling permits to minimize the dimension space of the primary variables by combining them into dimensionless groups, as follows:

$$\frac{M}{h^{5/2} \sqrt{G_F E_c}} = \Phi_1 \left( \frac{\sigma_u h^{1/2}}{\sqrt{G_F E_c}}, \rho_t \frac{\sigma_y h^{1/2}}{\sqrt{G_F E_c}}, \mathcal{G} \frac{E_c h^{1/2}}{\sqrt{G_F E_c}} \right) \quad (8)$$

if  $h$  and  $\sqrt{G_F E_c}$  are assumed as the dimensionally independent variables. It is worth noting that the former parameter is representative of the size-scale of the specimen, whereas the latter is a material property. In particular, the term  $\sqrt{G_F E_c}$  corresponds to the concrete fracture toughness,  $K_{IC}$ , according to the fundamental relationship proposed by Irwin (1957). As a consequence, the dimensionless functional relation for the proposed model becomes:

$$\tilde{M} = \Phi_2(s, N_p, \mathcal{G}_n) \quad (9)$$

where:

$$s = \frac{K_{IC}}{\sigma_u h^{1/2}} \quad (10)$$

and

$$N_p = \rho_t \frac{\sigma_y h^{1/2}}{K_{IC}} \quad (11)$$

are the governing nondimensional numbers,  $\tilde{M}$  is the nondimensional bending moment, and  $\mathcal{G}_n$  is the normalized local rotation. It is worth noting that Eq. (10), which represents the stress brittleness number introduced by Carpinteri (1981b, 1982), includes only the mechanical properties of the matrix and the size scale of the problem. On the other hand, Eq. (11) represents the reinforcement brittleness number introduced again by Carpinteri (1984) contextually with the Bridged Crack Model, and containing the properties of the reinforcement. As a result of the Dimensional Analysis, according to Eq. (9), the structural response, in terms of  $\tilde{M}$  versus  $\mathcal{G}_n$ , is a function of  $N_p$  and  $s$ .

#### 4 COMPARISON OF NUMERICAL PREDICTIONS AND EXPERIMENTAL RESULTS

The experimental investigation herein considered was carried out in the Materials and Structures Laboratory of the Department of Structural and Geotechnical Engineering of the Politecnico di Torino, by Bosco et al. (1990) with the main purpose of verifying the existence of size effects in the structural behavior. Thirty three-point-bending tests were performed on reinforced high-strength concrete beams. Three different size-scales have been considered, characterized by a depth,  $h$ , equal to 0.1, 0.2 and 0.4 m, and a constant thickness,  $b$ , equal to 0.15 m. The span to depth ratio was set equal to 6. The concrete properties were the following: cylindrical compressive strength  $\sigma_c = 76$  MPa, secant elastic modulus  $E_c = 34300$  MPa, and fracture energy  $G_F = 0.090$  N/mm. As regards the reinforcement, the nominal diameters of the adopted steel bars were 4, 5, 8 and

10 mm. The corresponding yield strengths were: 637, 569, 441 and 456 MPa. It is worth noting that the percentages were not assumed constant by varying the specimen size. On the contrary, they were varied keeping constant the brittleness number  $N_P$ , defined in Eq. (1).

Some of the numerical simulations compared to the corresponding experimental results, in terms of applied load vs. mid-span deflection curves, are shown in Figures 5 to 7. In the numerical simulations the RC element of Figure 1 is assumed to be representative of the mid-span portion of the beam subjected to the three-point-bending test. Hence, the mid-span deflection is obtained as the sum of the localized rotation contribution given by Eq. (5) and the elastic contribution, according to the following expression:

$$\delta = \delta_{loc} + \delta_{el} = \frac{gl}{4} + \frac{1}{48} \frac{Pl^3}{E_c J} \quad (12)$$

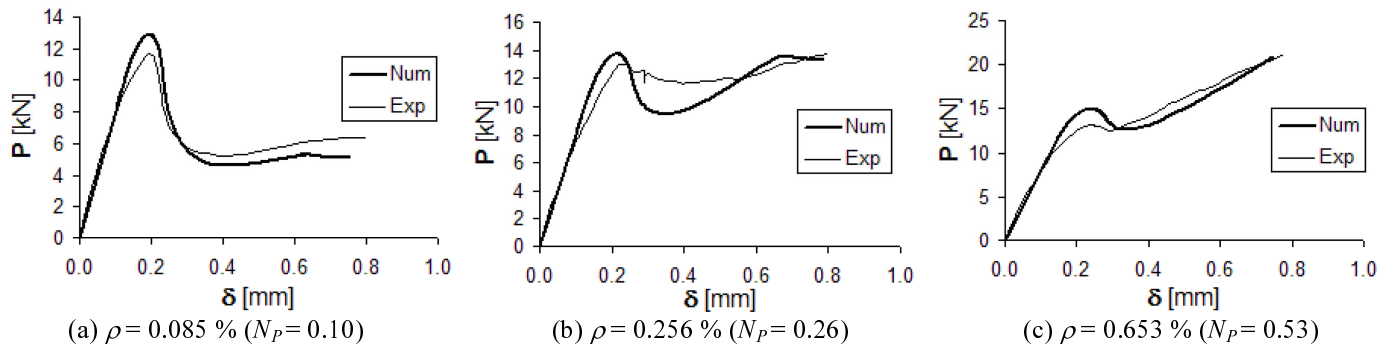


Figure 5. Comparison between numerical and experimental applied load vs. mid-span deflection curves for beam depth  $h = 0.2$  m.

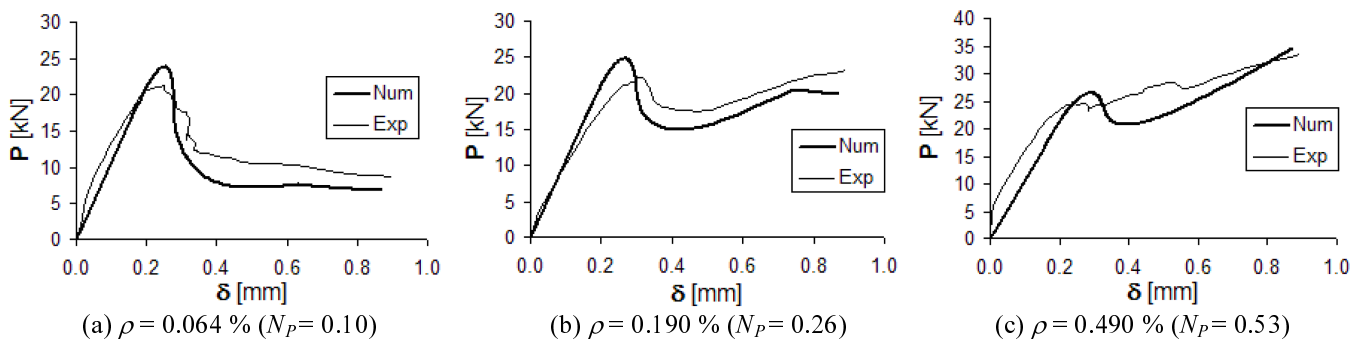


Figure 6. Comparison between numerical and experimental applied load vs. mid-span deflection curves for beam depth  $h = 0.4$  m.

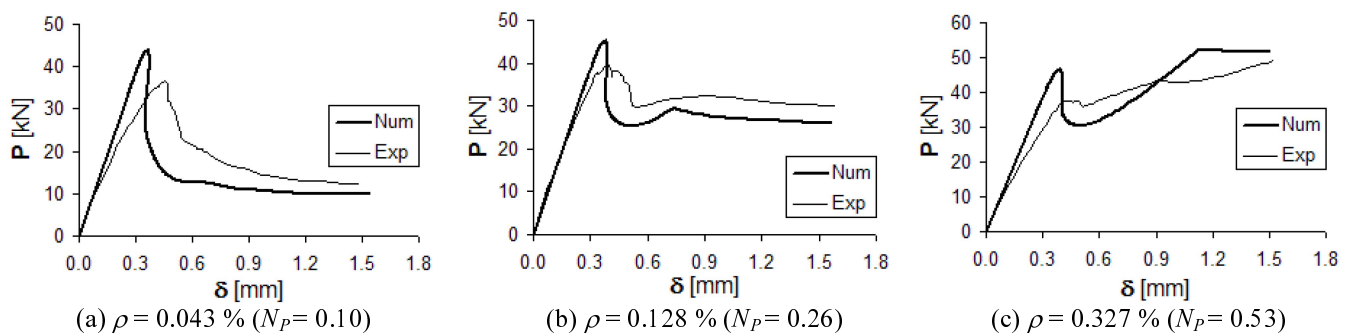


Figure 7. Comparison between numerical and experimental applied load vs. mid-span deflection curves for beam depth  $h = 0.6$  m.

where  $l$  is the beam span, and  $J$  is the moment of inertia of the cross-section. The curves in Figures 5 to 7 evidence a general good agreement between numerical and experimental results, although a linear softening law has been introduced in the cohesive model instead of a more complex relationship.

## 5 NUMERICAL RESULTS AND DISCUSSION

### 5.1 Parametric Analysis

In this section, according to the results of the dimensional analysis, the ductile-to-brittle transition in the structural response is analyzed on the basis of the two nondimensional numbers defined by Eqs. (10) and (11). The yielding strength and the elastic modulus of the steel reinforcement, as well as its relative distance from the tensile edge,  $c/h$ , are assumed, respectively, equal to 600 MPa, 200000 N/mm<sup>2</sup>, and 0.10, for all the numerical simulations. Also the beam width,  $b$ , is assumed to be constant and equal to 0.15 m. In this case, since the geometrical ratio  $b/h$  is no longer a constant, the expression of the nondimensional moment becomes:

$$\tilde{M} = \frac{M}{bh^{3/2}\sqrt{G_F E_c}} \quad (13)$$

The dimensionless moment versus normalized rotation curves shown in Figure 8 represent the mechanical behavior of RC beams characterized by values of  $N_p$  ranging from 0.00 up to 1.85, with  $s = 0.87$ . In general, the obtained curves are characterized by a first ascending branch, due to the elastic material behavior and to the initial stable crack propagation, up to the peak cracking moment, and then by a softening or even snap-back branch, due to an unstable crack propagation. Then, depending on the reinforcement amount, the loading process can return to be stable up to steel yielding. Finally, the mechanical response tends asymptotically to the ultimate moment, which corresponds to steel plastic flow and complete disconnection of the concrete cross-section. The diagrams in Figure 8 evidence an increment in the load-carrying capacity and a more ductile and stable mechanical behavior of the element by increasing  $N_p$ . More precisely, for the considered value of  $s$ , the global response becomes stable, i.e., the asymptotic value of the ultimate moment becomes higher than the peak cracking moment, when  $N_p$  is greater than 0.23 approximately.

The diagrams in Figure 9 show the dimensionless moment vs. normalized rotation relationships for different values of the stress brittleness number,  $s$ , ranging from 0.43 up to 2.63, with  $N_p = 0.28$ . We

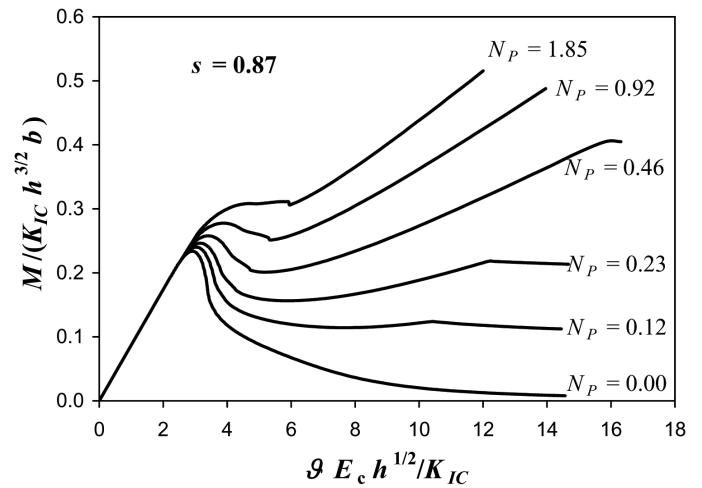


Figure 8. Numerical dimensionless moment vs. normalized rotation curves by varying  $N_p$  and for  $s = 0.87$ .

can observe that the value of the peak cracking moment, directly correlated to the concrete tensile strength, is a decreasing function of  $s$ . On the other hand, the post-peak branches collapse to the same asymptotic value of the ultimate bending moment, which is a function of steel content and yield strength. From a global point of view, a transition in the mechanical behavior from a very ductile and stable response to a brittle and unstable one, with the appearance of a snap-back instability, is evidenced by decreasing  $s$  from 2.63 to 0.43.

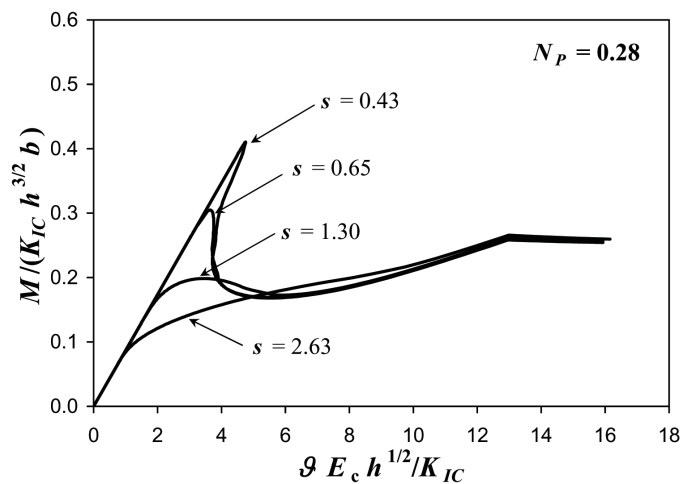


Figure 9. Numerical dimensionless moment vs. normalized rotation curves by varying  $s$  and for  $N_p = 0.28$ .

### 5.2 Minimum Reinforcement

In this section, a new relationship between the minimum reinforcement and the mechanical and geometrical parameters is proposed. To this aim, four different values of the beam depth,  $h = 0.1, 0.2, 0.4$  and  $0.8$  m, and five different values of the concrete grade,  $\sigma_c = 16, 30, 40, 65$ , and  $76$  MPa, have been considered. All the other mechanical properties of concrete, as, for instance, the tensile strength and

the fracture energy, have been evaluated according to the relationships provided by the Model Code 90. As regards the steel reinforcement, a yield strength  $\sigma_y = 600$  MPa, and an elastic modulus  $E_s = 200000$  MPa have been assumed. For each of the considered beams, several simulations have been carried out by varying the steel percentage, in order to find the minimum reinforcement amount. In particular, such a value is determined when the peak cracking load,  $P_{cr}$ , is equal to the ultimate load,  $P_u$ , as shown in Figure 10.

The values of  $s$  and  $N_p$  –in this case  $N_{PC}$ , since it contains the critical value of the reinforcement amount– corresponding to the critical conditions are shown in Figure 11. The obtained trend can be described with a very good approximation (goodness of fit  $r^2 = 0.999$ ) by the following hyperbolic curve:

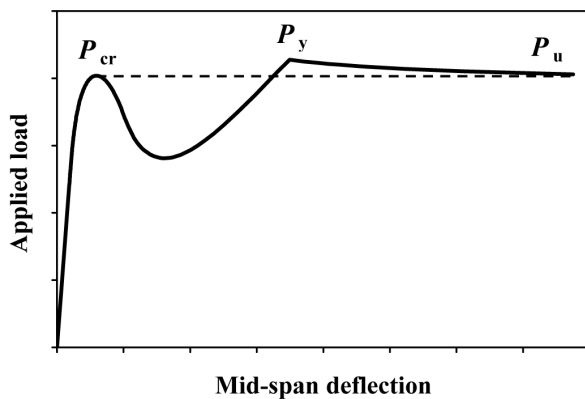


Figure 10. Definition of minimum reinforcement.

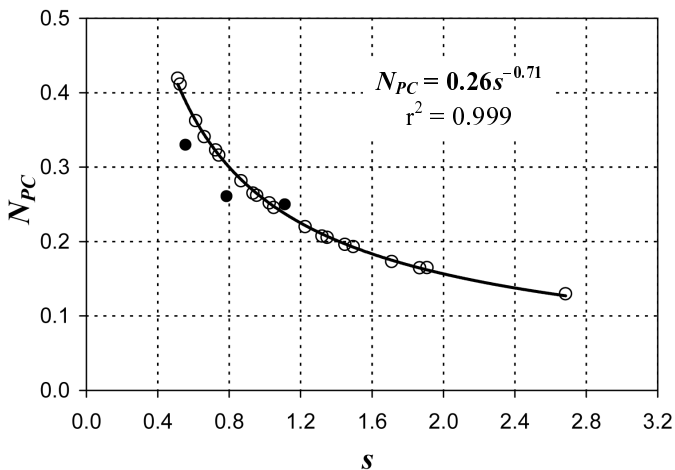


Figure 11. Best-fit relationship of numerical results (not filled-in symbols) between  $N_{PC}$  and  $s$ . Filled-in symbols refer to the experimental results from Bosco et al. (1990).

$$N_{PC} = 0.26s^{-0.71} \quad (14)$$

By substituting Eqs. (10) and (11) into (14), the following relationship between the minimum reinforcement and the mechanical and geometrical properties of the beam is obtained:

$$\rho_{\min} = 0.26 \left( \frac{\sigma_u h^{0.5}}{K_{IC}} \right)^{0.71} \frac{K_{IC}}{\sigma_y h^{0.5}} = 0.26 \frac{\sigma_u^{0.71} K_{IC}^{0.29}}{\sigma_y h^{0.15}}. \quad (15)$$

The minimum reinforcement percentage vs. beam depth curves according to the different models available in the literature are compared to Eq. (15) in Figure 12. All the curves refer to  $f_{ck} = 36.90$  MPa and  $\sigma_y = 450$  MPa. The relative distance between the reinforcement layer and the tensile cross-section edge has been kept constant and equal to 0.10 at any scale. Most of the curves clearly highlight a decrease in the minimum steel amount as the beam depth increases. The proposed curve is very close to that by Ruiz et al. (1999), but Eq. (15) is of easier practical applicability. The new proposed formula is also compared to the prescriptions of the design codes in Figure 13.

## 6 CONCLUSIONS

The application of Dimensional Analysis to the flexural behavior of lightly reinforced concrete beams permits the overall mechanical response to be governed only by two nondimensional numbers,  $N_p$  and  $s$ . In particular, the physical similitude in the nondimensional moment versus normalized rotation diagram predicted in the case the brittleness numbers are kept constant, is profitably used to select the minimum reinforcement amount. A new formula, in fact, is obtained a best-fitting the numerical results in terms of  $N_{PC}$  and  $s$ . In Eq. (15), the main mechanical and geometrical parameters affecting the phenomenon being studied are correctly taken into account by means of the Nonlinear Fracture Mechanics based model adopted for the numerical simulations. As a result, the minimum reinforcement amount is an increasing function of the concrete tensile strength and toughness, whereas it decreases as the steel yielding strength and the beam depth increase. The effect of the bond-slip between concrete and reinforcing bars pointed out by previous studies<sup>15,16</sup> is disregarded, since, with reference to Figure 10, it influences the value of the applied load and of the mid-span deflection corresponding to steel yielding,  $P_y$ , whereas  $P_{cr}$  and  $P_u$  do not considerably change.

As far as the size-scale effects are concerned, it has to be noted that the presence of cohesive closing stresses determines a variation in  $\rho_{\min}$  with the beam size less pronounced than that predicted by the *Bridged Crack Model*. An exponent equal to  $-0.15$ , in fact, is obtained instead of  $-0.50$ , typical of Linear Elastic Fracture Mechanics. Such a difference is clearly shown in Figure 12, where the curve from Bosco & Carpinteri (1992) is compared to the new proposal.

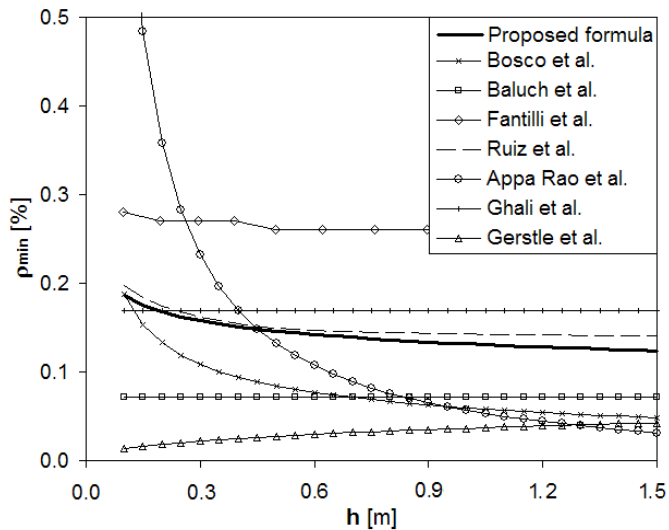


Figure 12. Minimum reinforcement vs. beam depth according to various models.

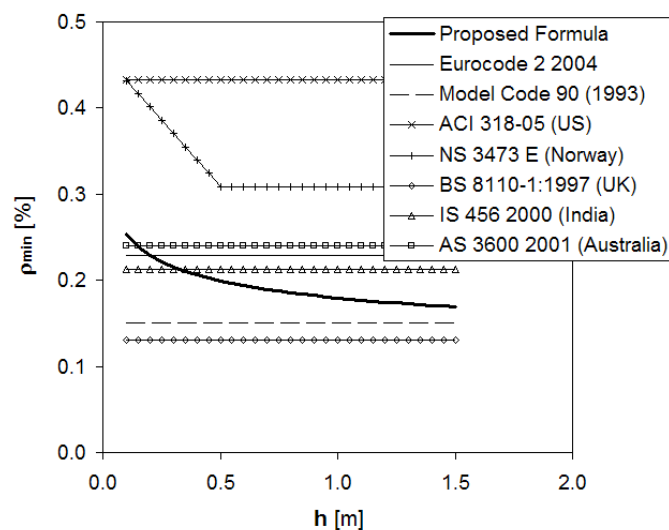


Figure 13. Minimum reinforcement vs. beam depth according to various design codes.

## REFERENCES

ACI-318 2005. *Building Code Requirements for Reinforced Concrete*. Detroit.

Appa Rao, G., Aravind, J. & Eligehausen, R. 2007 Evaluation of minimum flex. reinforcement in RC beams using fictitious crack approach. *Journal of Structural Engineering* (Madras) 34(4): 277-283.

Baluch, M., Azad, A. & Ashmawi, W. 1992. Fracture mechanics application to reinforced concrete members in flexure. In A. Carpinteri (ed), *Applications of Fracture Mechanics to Reinforced Concrete*: 413-436. London: Elsevier Applied Science.

Barenblatt, G.I. & Botvina, L.R. 1980. Incomplete self-similarity of fatigue in the linear range of fatigue crack growth. *Fatigue of Engineering Materials and Structures* 3(3): 193-202.

Bazant, Z.P. & Beissel, S. 1994. Smear-tip superposition method for cohesive fracture with rate effect and creep," *International Journal of Fracture* 65(3): 277-290.

Brincker, R., Henriksen, M.S., Christensen, F.A. & Heshe, G. 1999. Size effects on the bending behaviour of reinforced concrete beams. In A. Carpinteri (ed), *Minimum Rein-*

*forcement in Concrete Members*: 127-180. Oxford (UK): Elsevier Science Ltd.

BSI, BS 8110. 1997. *Code of practice for structural use of concrete*. London.

Buckingham, E. 1915. Model experiments and the form of empirical equations. *ASME Transaction* 37: 263-296.

Bosco, C. & Carpinteri, A. 1992. Fracture mechanics evaluation of minimum reinforcement in concrete structures. In A. Carpinteri (ed), *Applications of Fracture Mechanics to Reinforced Concrete*: 347-377. London: Elsevier Applied Science.

Bosco, C., Carpinteri, A. & Debernardi, P.G. 1990. Minimum reinforcement in high-strength concrete. *Journal of Structural Engineering* 116(2): 427-437.

Carpinteri, A. 1980. Size effect in fracture toughness testing: A dimensional analysis approach. In G.C. Sih, & M. Mirabile (eds), *Proceedings of an International Conference on Analytical and Experimental Fracture Mechanics*: 785-797. Alphen an den Rijn. Sijthoff & Noordhoff.

Carpinteri, A. 1981a. A fracture mechanics model for reinforced concrete collapse. In *Proceedings of a IABSE Colloquium*: 17-30. Delft: Delft University Press.

Carpinteri, A. 1981b. Static and energetic fracture parameters for rocks and concretes. *Materials & Structures* 14(81): 151-162.

Carpinteri, A. 1982. Notch sensitivity in fracture testing of aggregative materials. *Engineering Fracture Mechanics* 16: 467-481.

Carpinteri, A. 1984. Stability of fracturing process in RC beams. *Journal of Structural Engineering* 110(3): 544-558.

Carpinteri, A. 1985. Interpretation of the Griffith instability as a bifurcation of the global equilibrium. In S.P. Shah (ed), *Application of Fracture Mechanics to Cementitious Composites*: 287-316. Dordrecht: Martinus Nijhoff Publishers.

Carpinteri, A., Corrado, M., Paggi, M. & Mancini, G. 2007. Cohesive versus overlapping crack model for a size effect analysis of RC elements in bending. In A. Carpinteri, P. Gambarova, G. Ferro, & G. Plizzari (eds), *Fracture Mechanics of Concrete Structures*: 655-663. London: Taylor & Francis.

Carpinteri, A., Corrado, M., Paggi, M. & Mancini, G. 2009. New model for the analysis of size-scale effects on the ductility of reinforced concrete elements in bending. *Journal of Engineering Mechanics* 135(3): 221-229.

CEN TC/250 2004. *Eurocode 2: Design of Concrete Structures, Part 1-1: General Rules and Rules for Buildings*. Brussels.

Ciavarella, M., Paggi, M. & Carpinteri, A. 2008. One, no one, and one hundred thousand crack propagation laws: a generalized Barenblatt and Botvina dimensional analysis approach to fatigue crack growth. *Journal of the Mechanics and Physics of Solids* 56(12): 3416-3432.

Comité Euro-International du Béton. 1993. CEB-FIP Model Code 1990. In *Bulletin No. 213/214*. Thomas Telford Ltd, Lausanne.

Fantilli, A.P., Ferretti, D., Iori, I. & Vallini, P. 1999. Behaviour of R/C elements in bending and tension: the problem of minimum reinforcement ratio. In A. Carpinteri (ed), *Minimum Reinforcement in Concrete Members*: 99-126. Oxford (UK): Elsevier Science Ltd.

Gerstle, W.H., Dey, P.P., Prasad, N.N.V., Rahulkumar, P. & Xie, M. 1992. Crack growth in flexural members-A fracture mechanics approach. *ACI Structural Journal*: 89(6) 617-625.

Ghali, A., Favre, R. & Elbadry, M. 1986. *Concrete structures: stresses and deformations*, J. W. Arrowsmith Ltd., Bristol, UK, 1986.

- Hillerborg, A. 1990. Fracture mechanics concept applied to moment capacity and rotational capacity of reinforced concrete beams. *Engineering Fracture Mechanics* 35: 233-240.
- Hillerborg, A., Modeer, M. & Petersson, P.E. 1976. Analysis of crack formation and crack growth in concrete by means of fracture mechanics and finite elements. *Cement and Concrete Research* 6: 773-782.
- Jansen, D.C. & Shah, S.P. 1997. Effect of length on compressive strain softening of concrete. *Journal of Engineering Mechanics* 123(1): 25-35.
- Karihaloo, B.L. & Xiao, Q.Z. 2008. Asymptotic fields at the tip of a cohesive crack. *International Journal of Fracture* 150(1-2): 55-74.
- Norwegian Standard, NS 3473 E. 1989. *Concrete Structures, Design Rules*. (English Translation). Norwegian Council for Building Standardization, Oslo, Norway.
- Planas, J. & Elices, M. 1992. Asymptotic analysis of a cohesive crack: 1. Theoretical background. *International Journal of Fracture* 55(2): 153-177.
- Phatak, D.R. & Deshpande, N.P. 2005. Prediction of 28 days compressive strength of 53-grade cements using dimensional analysis. *Journal of Materials in Civil Engineering* 17(6): 733-735.
- Phatak, D.R. & Dhonde, H.B. 2003. Dimensional analysis of reinforced concrete beams subjected to pure torsion. *Journal of Structural Engineering* 129(11): 1559-1563.
- Ruiz, G., Elices, M. & Planas, J. 1999. Size effects and bond-slip dependence of lightly reinforced concrete beams. In A. Carpinteri (ed), *Minimum Reinforcement in Concrete Members*: 127-180. Oxford (UK): Elsevier Science Ltd.
- Standards Australia, AS-3600. 2001. *Australian Standard for Concrete Structures*. Sydney.
- Suzuki, M., Akiyama, M., Matsuzaki, H. & Dang, T.H. 2006. Concentric loading test of RC columns with normal- and high-strength materials and averaged stress-strain model for confined concrete considering compressive fracture energy. In *Proceedings of the 2nd fib Congress*, Naples, Italy, June 5-8, 2006, (CD-ROM).
- van Mier, J.G.M. 1984. *Strain-softening of Concrete under Multiaxial Loading Conditions*. PhD Thesis, Eindhoven University of Technology.